Available online at www.sciencedirect.com
SCIENCE DIRECT®
Optical Materials 28 (2006) 473–479
OPTICAL Materials
www.elsevier.com/locate/optmat

Optical properties of amorphous diamond films evaluated by non-destructive spectroscopic ellipsometry

Jiaqi Zhu *, Jiecai Han, Xiao Han, Songhe Meng, Aiping Liu, Xiaodong He

Center for Composite Materials, Harbin Institute of Technology, P.O. Box 3010, Yikuang Street 2, Harbin 150001, China

Received 10 October 2004; accepted 11 April 2005
Available online 1 June 2005

Abstract

In order to investigate the regularities between the optical properties and the deposition conditions, the optical constants of amorphous diamond films deposited at the different substrate bias with the filtered cathodic vacuum arc technology have been measured by spectroscopic ellipsometry. It has been found that the refractive index and the optical gap of the films firstly increase and then decrease with the enhancing bias and there are respectively the maximal values when the negative bias is 80 V. However, the extinction coefficient of the films firstly minishes and then rises with the adding bias and there is the minimal value when the negative bias is also 80 V. The extinction coefficient gradually drops down with the increasing wavelength of incident light and nearly approaches to zero in the infrared band. Moreover, the adjustable scopes of refractive index and extinction coefficient changed by the substrate bias deflate little by little with the adding wavelength of incident light.

PACS: 78.66.B

Keywords: Amorphous diamond; Filtered cathodic vacuum arc; Spectroscopic ellipsometry; Optical properties

1. Introduction

In contrast with hydrogenated amorphous carbon (α-C:H), amorphous diamond (α-D) or tetrahedral amorphous carbon (ta-C) is characterized by the better heat stability and the better mechanical, optical and electrical properties. In comparison with diamond films, α-D films with the adjustable microstructure and performance possess the higher applicable value since the films with the smooth surface are able to be prepared on the greater area at the ambient temperature [1–3]. It is attractive especially that α-D films have the potential uses as the protective coatings, the anti-reflexion films and the passivation layers of many infrared optical devices because of the transparence in the wide band [4,5]. In addition, both the basic studies and the applied oriented research of α-D films attempt to characterize the optical constants (refractive index and extinction coefficient), optical gap, electronic density of states and the ratio of different hybridizations [6]. The necessary means to investigate the optical properties of α-D films have been provided due to the extension of spectroscopic ellipsometry [7]. In this work, the optical constants of α-D films deposited by the filtered cathodic vacuum arc technology were measured by spectroscopic ellipsometry, and furthermore, the effectual regularity of deposition process was analyzed.

2. Experimental

The samples were prepared with the filtered cathodic vacuum arc technology whose working mechanism and

* Corresponding author. Tel.: +86 451 86417970; fax: +86 451 86414145.
E-mail address: zhujq@hit.edu.cn (J. Zhu).

0925-3467/$ - see front matter © 2005 Elsevier B.V. All rights reserved.
doi:10.1016/j.optmat.2005.04.008

systematic details had been described elsewhere [8,26]. A series of specimens of α-D films with the same film thickness were deposited under the different pulse negative substrate bias from 0 to 2000 V. The pulse frequency was fixed at 2500 Hz and the pulse width was 25 μs. To smoothen the cathodic target surface and stabilize the process, the striker assembly ignited mechanically the arc once every 15 s. Before deposition, the bare p-type (1 0 0) c-Si substrate was rinsed with acetone in a supersonic sink for 15 min and then was etched with Kaufman Ar^+ ion gun for 5 min. To ensure the uniformity, the substrate disc holder rotated at the rate of 33 r/min during deposition and etching.

The optical data were derived using the variable angle spectroscopic ellipsometer (VASE) manufactured by J.A. Woollam Company. The ellipsometric parameters were measured in the spectral scope 240–1700 nm with the incidence angles of 55°, 65°, 75°. The diameter of the polarization light beam was 3 mm and the packed Si/InGaAs detector examined the polarization state of the reflected beam. The whole experimental process was done using the standard apparatus software. The ratio of the different hybridization was acquired using Philips Tecnai F30 analytical TEM equipped with Gatan-666 parallel-detection EELS.

3. Theoretical considerations

Fig. 1 shows the essential optical physics of ellipsometry [7]. The measured change in polarization state (both amplitude ψ and phase Δ) of the reflected beam can be used to deduce the optical properties of the films. Since light wave is transversal wave, the electric field of incident linearly polarized light can be decomposed into the two perpendicular vector components, i.e. p-plane and s-plane constituents. The reflected light is also done in the same manner. According to Eq. (1), the Fresnel reflection coefficient ρ is represented as the quotient of the p-plane component R_P divided by the s-plane component R_S. They are all complex numbers.

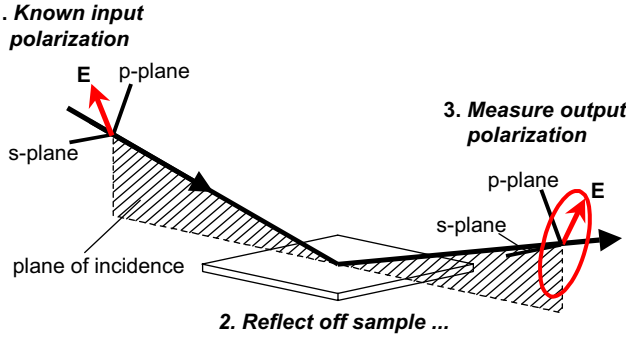

Fig. 1. The schematic geometry of ellipsometry measurement.

$$\rho = \frac{R_P}{R_S} = \tan(\psi)e^{i\Delta}. \tag{1}$$

By means of the boundary conditions between the different media, the mathematical expressions of R_P and R_S can be deduced from Maxwell's equations [shown in Eqs. (2) and (3)]. Wherein θ_0 and θ_1 is respectively the incident angle and the refractive angle, while N_0 and N_1 is respectively the complex refractive index of air and the one of the films.

$$R_P = \frac{N_1 \sin\theta_0 - N_0 \sin\theta_1}{N_1 \cos\theta_0 + N_0 \cos\theta_1}, \tag{2}$$

$$R_S = \frac{N_0 \cos\theta_0 - N_1 \cos\theta_1}{N_0 \cos\theta_0 + N_1 \cos\theta_1}. \tag{3}$$

In light of Snell refractive law and the parity of complex number, the correlations between the optical constants (refractive index n and extinction coefficient k) and the polarized parameters (amplitude ψ and phase Δ) can be derived [9]. They are shown in Eqs. (4) and (5).

$$n = \left\{ k^2 + n_0^2 \sin^2\theta_0 \times \left[1 + \frac{\tan^2\theta_0(\cos^2 2\psi - \sin^2 2\psi \sin^2\Delta)}{(1 + \sin 2\psi \cos\Delta)^2} \right] \right\}^{\frac{1}{2}}, \tag{4}$$

$$k = \frac{n_0^2 \sin^2\theta_0 \tan^2\theta_0 \sin 4\psi \sin\Delta}{2n(1 + \sin 2\psi \cos\Delta)^2}. \tag{5}$$

The optical properties of a medium can be conveniently expressed in terms of the complex index of refraction (Eq. (6)) due to the research motive, wherein N, n and k are all real functions of photon frequency ω. The real part and imaginary part of the complex refractive index are connected together with the general Kramers–Kronig dispersion relations [10].

$$N(\omega) = n(\omega) + ik(\omega). \tag{6}$$

The deeper the light propagates into the films, the more energy will be absorbed. How much is absorbed is determined by the extinction coefficient k or the absorption coefficient α and the exponential decay relationship on the foundation of Beer's law shown in Eq. (7) [11]. Wherein I_0 is the initial light intensity, x is the propagation depth and λ is the wavelength.

$$I = I_0 e^{-\alpha x}, \quad \alpha = \frac{4\pi k}{\lambda}. \tag{7}$$

In amorphous semiconductors it is normally assumed that the electronic density of states just beyond the band edges has a parabolic dependence on photon energy [12]. Eq. (8) represents the excitation spectra at the absorption edge and defines the optical gap E_0.

$$\sqrt{\alpha h\omega} = B(h\omega - E_0). \tag{8}$$

4. Results and discussion

4.1. Refractive index

Fig. 2 shows the dispersion dependence to the refractive index of α-D films deposited at the different substrate bias. When the photon energy is higher, the refractive index changes strikingly with the increasing wavelength. However, the refractive index of the different films is almost constant with the wavelength in the visible and infrared band. The refractive index of the films except deposited under the floating conditions is about in the range 2.6–2.7 and is greater than the one of crystal diamond (the refractive index of I-type diamond prepared with CVD process is 2.42 [13]) and the other α-D films [6,14]. It is well known that light rate in a vacuum is the greatest ($c = 3 \times 10^8$ m/s) and refractive index is a measure of the amount of impedance to the propagation of light for a certain material. Light travels at the speed of c/n through a different medium. In this qualitative sense, refractive index is the optical "density" of a material and is determined by the atomic density and the dipole matrix [10,15]. In fact, the refractive index of α-D films is generally greater than the one of diamond [6,14,16–18]. It is apparent that this phenomenon cannot be illuminated at the base of atomic density. Since the atomic structure of α-D films is a concordant entity composed of sp^2 and sp^3 hybridizations like α-Si or α-Ge [19,20], the polarization actions that are distinct from the ones of crystal diamond will be generated when light travels in such an amorphous framework. It should be emphasized that the discrete π locations within the σ bonding matrix work prominently on the optical and electronic properties of α-D films. The optical differences of the diverse α-D films are just owing to the multiformities of distribution and contents of π states. In additional, the refractive index of α-D films is generally more than the one of hydrogenated amorphous carbon (α-C:H), however, the adjustive scope of the refractive index is less much than the one of the refractive index of α-C:H. Hydrogen is important to stabilize the tetrahedral bonds and to control the properties of α-C:H films. The content of hydrogen can be varied in the range 1–60%, therefore, the refractive index can be adjusted in a wide range 1.6–2.6 [21–24]. The mass of hydrogen atom is the least and the scattering for the photon is likewise the feeblest, moreover, it is difficult to control the energy of the products decomposed from the hydrocarbon precursor so that the coatings are loose and low-density. Accordingly, the refractive index of α-C:H films is less than the one of α-D films.

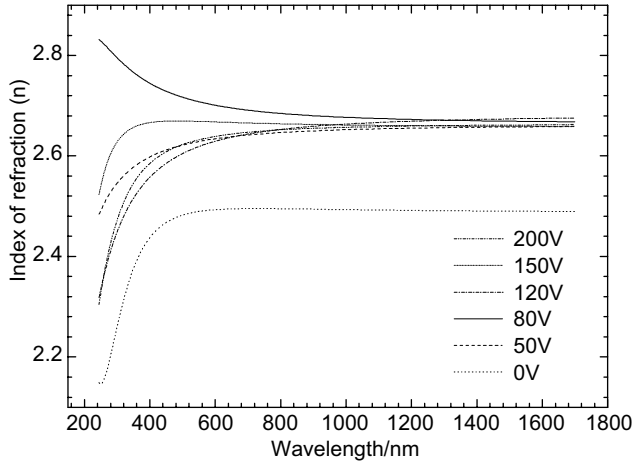

Fig. 2. The real refractive index of α-D films deposited at different bias vs. the wavelength of incident polarized light.

From Fig. 3, we can see that the refractive index of α-D films firstly hoists and then drops with the increasing substrate bias and there is the maximal value when the negative bias is 80 V. When the photon energy is higher, the refractive index of the films deposited at the varied bias is markedly different. The adjustable scope of refractive index by the changing bias gradually reduces with the lengthening wavelength of the incident light. In other words, the adjustability of refractive index in the infrared band is limited. The variation of refractive index is attributed mainly to the optical dispersion relations of the amorphous framework when the energy of incident photon is less than the optical gap [25]. In addition, refractive index takes the maximal value exactly at the sp^3-rich energy window [26]. The more the content of sp^3 hybridization is, the higher refractive index of the films is. This rule is just contrasted with the results of Lossy [27] and Chen [18]. The higher the proportion of sp^3 hybridization is, the more α-D films approach to crystal diamond. As the refractive index of crystal diamond is 2.42, they thought the refractive index of α-D films descends firstly and then elevates again with the increase of the impinging energy. Maybe the discrepancies are on account of the different deposition systems. However, it just illustrates the complexity of the interaction between incident photon and amorphous framework. The horizontal axis about the substrate bias only indicate the pre-setup values of the digital programmable power supply with a high voltage pulse generator in the deposition system. In practice, the substrate will have the same potential as the plasma beam and the kinetic energy of the C^+ reaching the substrate will possess certain original ion energy (about 20–30 eV) under the floating conditions [27–29].

4.2. Extinction coefficient

Fig. 4 shows that the extinction coefficients of α-D films lessen gradually with the increasing wavelength of the incident light and nearly approach to zero in the infrared band. The changing tendency is often taken

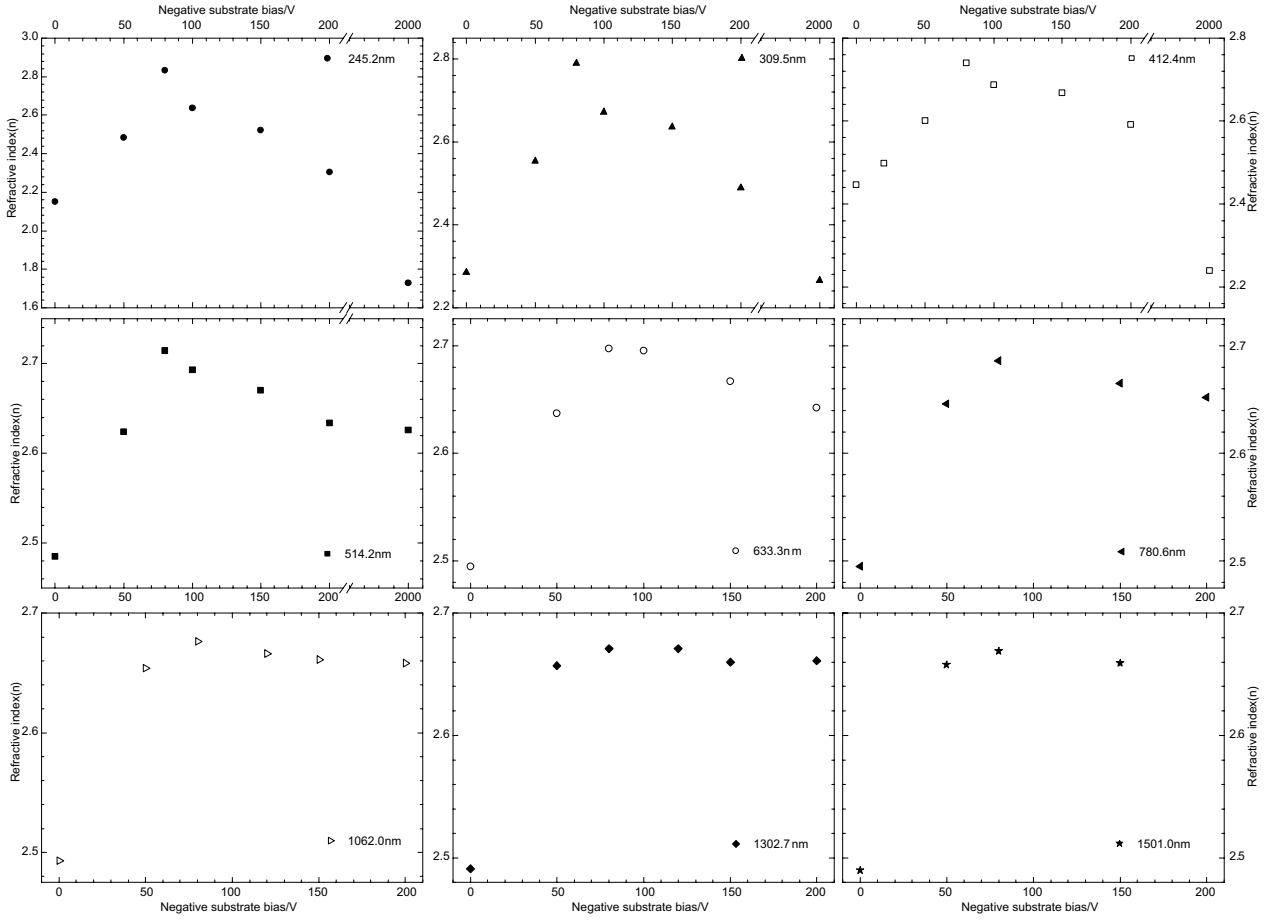

Fig. 3. Refractive index of α-D films at different wavelength vs. negative substrate bias. The adjustable scope of refractive index by the changing bias gradually reduces with the lengthening wavelength of the incident light. The 0 V labeled on the *x*-axis only means that the presetup value of high pulse bias is zero.

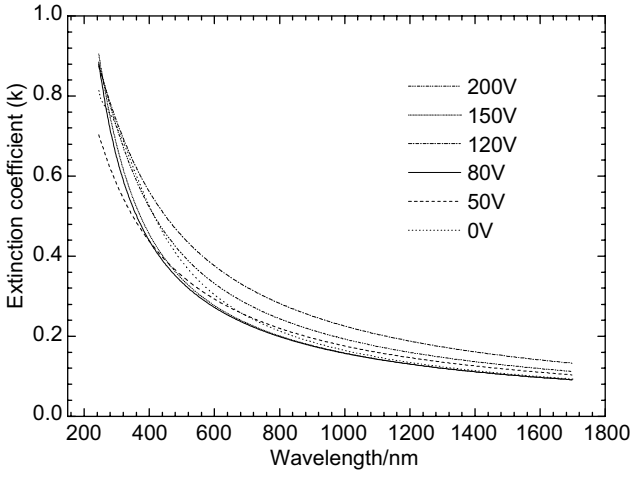

Fig. 4. The extinction coefficient of α-D films deposited at different substrate bias vs. the wavelength of incident polarized light.

as one of the criteria estimating whether the ellipsometric data have been fitted successfully. The films are opaque or subtransparent in the ultraviolet band because of the greater extinction coefficient. In the visible range, the extinction coefficient has evidently fallen down so that the films are subtransparent even transparent. The films appear from light brown to light black with the accumulating film thickness as a result of the wave interference. The extinction coefficient is so tiny that the films are completely lucid in the infrared band. Just by means of the outstanding properties, α-D films can be taken advantage of as the antireflective and protective coatings for some infrared optical windows or devices [4,5]. In fact, the extinction coefficients in Fig. 4 are not very perfect because charge accumulation emerged during deposition due to the insulation between the substrate and the holder. This problem has also been met in the other experiments [6].

In order to investigate the correlations between extinction coefficient and the deposition conditions, Fig. 5 has been plotted at the different incident wavelength. The extinction coefficient of α-D films demonstrates a U-shaped trace with the increasing substrate bias. When the negative bias is 80 V, the extinction coefficient is the minimal. When the wavelength of the inci-

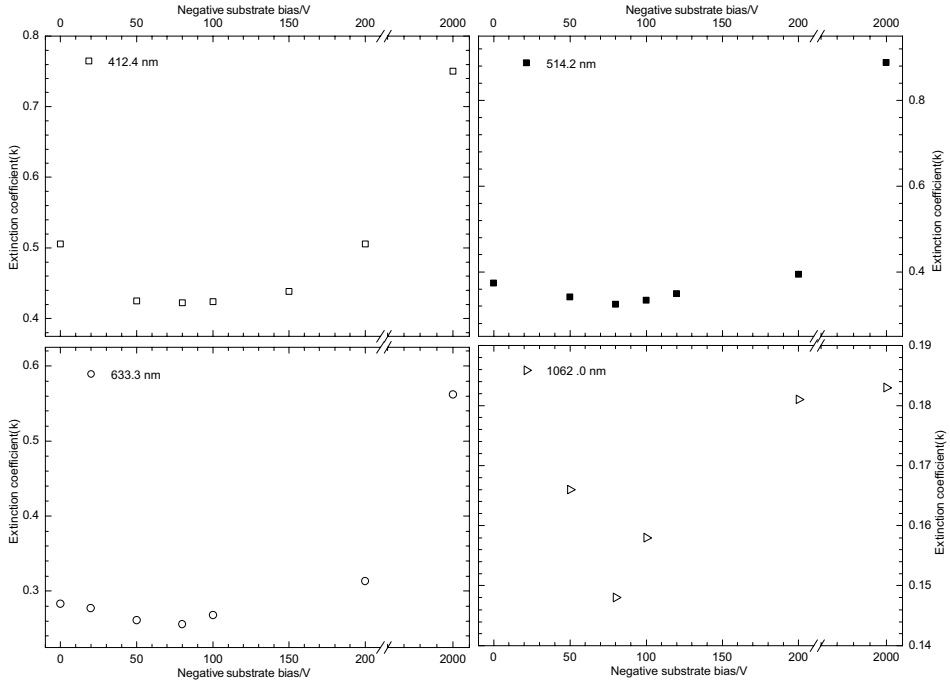

Fig. 5. Extinction coefficient of α-D films at different wavelength vs. Negative substrate bias. When the wavelength of the incident light extends to the infrared band, the changing amplitude of extinction coefficient under the varied bias obviously lessens also.

dent light extends to the infrared band, the changing amplitude of extinction coefficient under the varied bias obviously lessens also. For example, the difference of extinction coefficient is nearly equal to 0.35 when the wavelength of incident light is 412.4 nm, however, the difference is less than 0.05 when the wavelength is 1 μm. In addition, there are no evident changing functions for extinction coefficient in the ultraviolet range due to the complex band-to-band transitions of α-D films.

4.3. Optical gap

In the amorphous materials, the optical absorption curve generally consists of three parts, i.e. the high absorptive zone, the exponential absorptive zone and the low absorptive zone [30]. We are interested in the high absorptive zone that ascertains the optical absorption edge corresponding to the interband transition. According to the lineshapes of the absorption curves, the measured absorptive spectra of α-D films should be ascribed to the high absorptive zone and the exponential absorptive zone. Since the connections between the absorptive coefficient and the energy of incident photon have been affirmed in Eq. (8), the Tauc gap, E_0, could be calculated and has been plotted in Fig. 6. The dependence of optical gap (E_0) on the substrate bias tally well with the dependencies of mechanical properties and surface morphology on the substrate bias [8, 26].

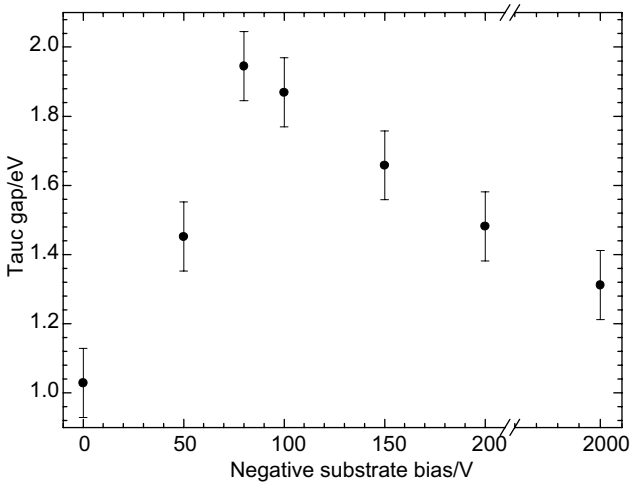

Fig. 6. Tauc gap of α-D films vs. Negative substrate bias. When the negative bias is 80 V, E_0 is the maximal.

Fig. 7 has exhibited clearly the trend of an E_0 increase as the sp^3 faction hoists. The gradual change is shared at the same time with the other types of amorphous carbon [31–33]. The regularity can be easily understood in light of the subplantation growth model for the α-D films [34]. The inset shows that the optimum substrate bias for the sp^3-rich films is −80 V. The certain energy is necessary for the impinging species to penetrate the surface. The ion flux with appropriate energy will create the local densification under a few carbon layers from the surface

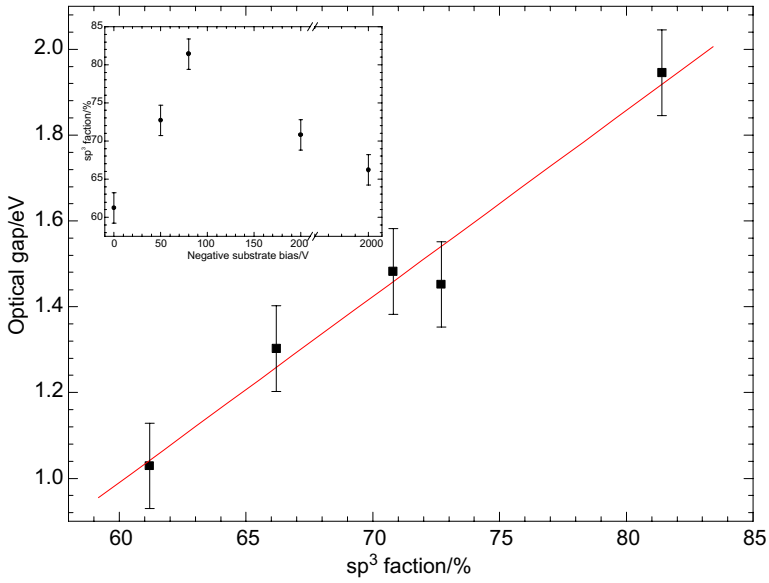

Fig. 7. Optical (Tauc) gap changes as a function of sp^3 faction determined by EELS. The light line guiding the eyes suggests that there is the almost linear relation between the optical gap and the sp^3 content. The inset shows that the sp^3 content is the most at −80 V.

and form the most tetrahedral hybridization. But any excess energy will be evolved as heat and allow a relaxation of the density increment. The more sp^3 content is, the more transparent the films are. The most sp^3 bonding can contribute to the highest optical band gap and the lowest extinction coefficient. Moreover, the refractive index is also the maximal because of the highest film density. If the sp^3 content reduces when the ion energy deviates from the optimum condition, the optical band gap will decrease and the extinction coefficient will also increase correspondingly. In practice, the optical properties are determined mainly by the sp^2 sites embedded in the rigid tetrahedral matrix because the density of states for π bonding is closer to the Fermi level. The trend of the band gap increase as the sp^3 faction hoists might be attributed to the π bands narrower and the π–π^* gap widens as the sp^2 content decreases [31].

5. Conclusions

The optical properties of α-D films deposited by filtered arc have been investigated by spectroscopic ellipsometry in this work. It has been shown that there are evident dependencies of refractive index, extinction coefficient and optical gap on the deposition conditions. The refractive index and the optical gap of the films firstly increase and then decrease with the enhancing bias and there are respectively the maximal values when the negative substrate bias is 80 V. However, the extinction coefficient of the films firstly minishes and then rises with the adding bias and there is the minimal value when the negative bias is 80 V. The extinction coefficient gradually falls down and is nearly close to zero with the lengthening wavelength of incident light. In addition, the adjustable scopes of refractive index and extinction coefficient by the changing deposition conditions lessen step by step with the extension of the wavelength.

References

[1] W.I. Milne, J. Non-cryst. Solids 198–200 (1996) 605.
[2] J. Hong, A. Goullet, G. Turban, Thin Solid Films 364 (2000) 144.
[3] S.G. Wang, Q. Zhang, S.F. Yoon, J. Ahn, Q. Wang, D.J. Yang, Q. Zhou, N.L. Yue, Opt. Mater. 24 (2003) 509.
[4] J. Ishikawa, Y. Takeiri, K. Ogawa, T. Takagi, J. Appl. Phys. 61 (1987) 2509.
[5] F. Davanloo, E.M. Juengerman, D.R. Jander, T.J. Lee, C.B. Collins, J. Appl. Phys. 67 (1990) 2081.
[6] Y. Lifshitz, G.D. Lempert, E. Grossman, H.J. Scheibe, S. Voellmar, B. Schultrich, A. Breskin, R. Chechik, E. Schefer, D. Bacon, R. Kalish, A. Hoffman, Diamond Related Mater. 6 (1997) 687.
[7] B. Johs, J.A. Woollam, C.M. Herzinger, J. Hilfiker, R. Synowicki, C.L. Bungay, SPIE CR72 (1999) 29.
[8] J. Zhu, J. Wang, S. Meng, J. Han, L. Zhang, Acta Phys. Sinica 53 (4) (2004) 1150 (in Chinese).
[9] Y.B. Liao, Polarizational Optics, Science Press, Beijing, 2003, 322-328, (in Chinese).
[10] T. Musienko, V. Rudakov, L. Solov'ev, J. Phys. Condens. Matter. 1 (1989) 6745.
[11] W. Frederick, Optical Properties of Solids, Academic Press, New York, 1972.
[12] J. Tauc, A. Menth, J. Non-Cryst. Solids 8–10 (1972) 569.
[13] W.J. Tropf, T.J. Harris, M.E. Thomas, Optical materials: visible and infrared, in: R.W. Waynant, M.N. Ediger (Eds.), Electro-Optics Handbook, 2nd Edition., McGraw-Hill Press, Columbus, 2000, 11.29.
[14] X.W. Zhang, W.Y. Cheung, N. Ke, S.P. Wong, J. Appl. Phys. 92 (3) (2002) 1242.
[15] J. Robterson, Mater. Science and Engineering:R 37 (4–6) (2002) 129.

[16] A. Canillas, M.C. Polo, J.L. Andujar, J. Sancho, S. Bosch, J. Robertson, W.I. Milne, Diamond Related Mater. 10 (2001) 1132.
[17] B.K. Tay, X. Shi, L.K. Cheah, D.I. Flynn, Thin Solid Films 308–309 (1997) 268.
[18] Z.Y. Chen, J.P. Zhao, J. Appl. Phys. 87 (9) (2000) 4268.
[19] P.H. Gaskell, A. Saeed, P. Chieux, D.R. McKenzie, Phys. Rev. Lett. 67 (1991) 1286.
[20] N.A. Marks, D.R. McKenzie, B.A. Pailthorpe, Phys. Rev. Lett. 76 (1996) 768.
[21] W.A. McGahan, T. Makovicka, J. Hale, J.A. Woollam, Thin Solid Films 253 (1994) 57.
[22] S. Choi, K.R. Lee, S. Oh, S. Lee, Appl. Surf. Sci. 169–170 (2001) 217.
[23] F.W. Smith, J. Appl. Phys. 55 (3) (1984) 764.
[24] D.S. Patil, K. Ramachandran, N. Venkatramani, M. Pandey, R. D'Cunha, Pramana-J. Phys. 55 (2000) 933.
[25] A.R. Forouhi, I. Bloomer, Phys. Rev. B 36 (10) (1986) 7018.
[26] J.Q. Zhu, J.C. Han, S.H. Meng, Q. Li, M.L. Tan, J. Mater. Sci. Technol. 19 (Supp l.1) (2003) 109.
[27] R. Lossy, D.L. Pappas, R.A. Roy, J.P. Doyle, J.J. Cuomo, J. Bruley, J. Appl. Phys. 77 (9) (1995) 4750.
[28] Shi Xu, B.K. Tay, H.S. Tan, Li Zhong, Y.Q. Tu, S.R.P. Silva, W.I. Milne, J. Appl. Phys. 79 (1996) 7234.
[29] P.J. Martin, S.W. Filipczuk, R.P. Netterfield, J.S. Field, D.F. Whitnall, D.R. McKenzie, J. Mater. Sci. Lett. 7 (1988) 410.
[30] M.H. Brodsky, Amorphous Semiconductors, Springerg-Verlag, Berlin, 1979.
[31] C. Oppedisano, A. Tagliaferro, Appl. Phys. Lett. 75 (1999) 3650.
[32] J. Robertson, Phys. Rev. B 53 (1996) 16302.
[33] N. Savvides, J. Appl. Phys. 58 (1985) 518.
[34] Y. Lifshitz, S.R. Kasi, J.W. Rabalais, W. Eckstein, Phys. Rev. B 41 (1990) 10468.